Rab27a Regulates the Peripheral Distribution of Melanosomes in Melanocytes

Alistair N. Hume,* Lucy M. Collinson,‡ Andrzej Rapak,* Anita Q. Gomes,* Colin R. Hopkins,‡ and Miguel C. Seabra*

*Cell and Molecular Biology Section, Division of Biomedical Sciences and ‡Department of Biochemistry, Imperial College of Science, Technology and Medicine, London SW7 2AZ, United Kingdom

Abstract. Rab GTPases are regulators of intracellular membrane traffic. We report a possible function of Rab27a, a protein implicated in several diseases, including Griscelli syndrome, choroideremia, and the Hermansky-Pudlak syndrome mouse model, *gunmetal*. We studied endogenous Rab27a and overexpressed enhanced GFP-Rab27a fusion protein in several cultured melanocyte and melanoma-derived cell lines. In pigmented cells, we observed that Rab27a decorates melanosomes, whereas in nonpigmented cells Rab27a colocalizes with melanosome-resident proteins. When dominant interfering Rab27a mutants were expressed in pigmented cells, we observed a redistribution of pigment granules with perinuclear clustering. This phenotype is similar to that observed by others in melanocytes derived from the *ashen* and *dilute* mutant mice, which bear mutations in the *Rab27a* and *MyoVa* loci, respectively. We also found that myosinVa coimmunoprecipitates with Rab27a in extracts from melanocytes and that both Rab27a and myosinVa colocalize on the cytoplasmic face of peripheral melanosomes in wild-type melanocytes. However, the amount of myosinVa in melanosomes from Rab27a-deficient *ashen* melanocytes is greatly reduced. These results, together with recent data implicating myosinVa in the peripheral capture of melanosomes, suggest that Rab27a is necessary for the recruitment of myosinVa, so allowing the peripheral retention of melanosomes in melanocytes.

Key words: Rab27a • GTP-binding proteins • vesicular transport • melanosome • myosinVa

Introduction

Rab proteins are GTPases that control intracellular vesicular transport (Novick and Zerial, 1997; Chavrier and Goud, 1999). Rabs form the largest family within the Ras superfamily, as >50 members have been recognized in mammalian cells to date (Pereira-Leal and Seabra, 2000). Many Rabs have a characteristic subcellular localization and are proposed to regulate specific steps in intracellular trafficking. The best characterized function of Rabs is to promote docking and fusion of vesicles between specific pairs of vesicle donor and organelle acceptor membranes (Novick and Zerial, 1997; Schimmöller et al., 1998). This function seems to be accomplished by recruitment of tethering factors, an apparently diverse group of proteins that bring the transport vesicle into close proximity to the acceptor membrane (Pfeffer, 1999). There is also evidence to support their involvement in vesicle formation (for review see Woodman, 1998).

Recently, several studies have suggested that Rabs also interact with cytoskeletal elements and influence the movement of intracellular membrane vesicles and tubules. A direct interaction between Rab6 and Rabkinesin6, a kinesin-like molecule, may stimulate the movement of Golgi retrograde transport vesicles towards the plus-end of microtubules, i.e., to the periphery of the cell where they fuse with ER membranes (Echard et al., 1998). In budding yeast, activation of Sec4p by the guanine nucleotide exchange factor Sec2p appears to be an important step, allowing the movement of secretory vesicles along the polarized actin cytoskeleton towards the daughter bud (Walch-Solimena et al., 1997). Overexpression of Rab8 results in changes in cell shape and rearrangement of both the actin and microtubule cytoskeleton (Peranen et al., 1996), whereas Rab5 is proposed to promote the motility of early endosomes on microtubules (Nielsen et al., 1999). Finally, Rab3d may regulate the actin coating of zymogen granules in the exocrine pancreas and thereby facilitate their movement across the subapical actin cytoskeleton towards the site of exocytosis (Valentijn et al., 2000).

The online version of this article contains supplemental material.

Address correspondence to Miguel C. Seabra, Cell and Molecular Biology Section, Division of Biomedical Sciences, Imperial College School of Medicine, Sir Alexander Fleming Building, London SW7 2AZ, UK. Tel.: 44-20-7594-3024. Fax: 44-20-7594-3015. E-mail: m.seabra@ic.ac.uk

Some Rabs such as Rab1 and Rab5 are ubiquitous and function in common steps in the exocytic and endocytic pathways of all mammalian cells. Other Rabs appear more tissue restricted, suggesting a more specialized function. The Rab27 proteins are an example of the latter. Rab27a is enriched in eye, platelets, skin, lung, spleen, intestine, and pancreas (Seabra et al., 1995; Chen et al., 1997). Both Rab27a and Rab27b isoforms were isolated from melanocyte, platelet, and megakaryocyte cells, suggesting an important function in these cell types and in diseases that affect them (Nagata et al., 1990; Seabra et al., 1995; Chen et al., 1997). One of these diseases, manifested by partial albinism and hemorrhagic disease, is Hermansky-Pudlak syndrome (HPS)[1] (Shotelersuk and Gahl, 1998; Spritz, 2000). HPS may be caused by defects in the biogenesis/maturation/secretion of specialized organelles of common endolysosomal origin, such as the melanosomes in melanocytes and the dense granules in platelets (Jackson, 1997; Swank et al., 1998).

Melanocytes reside in the basal level of the epidermis at the base of hair follicles and possess many long dendrites that allow intercellular transport of pigment containing melanosomes from the cell body, the site of synthesis, to surrounding keratinocytes (for review see Jackson, 1994). Melanosomes are related to lysosomes, as both are acidic and thought to contain lysosome-associated membrane protein (LAMP) family proteins (Orlow et al., 1993). However, melanosomes may be characterized morphologically on the basis of their ellipsoidal appearance and internal membrane striations, and biochemically due to the presence of matrix proteins (e.g., silver protein/Pmel17/gp100) and enzymatic proteins (e.g., tyrosinase and tyrosine-related protein 1 [TRP-1]/gp75) (Orlow et al., 1993; Lee et al., 1996). The biogenesis/maturation of melanosomes in melanocytes is divided into four stages, each with distinct morphological and biochemical characteristics (for review see Jimbow et al., 2000). In summary, structural and enzymatic proteins of the melanosome are processed through the ER and Golgi and sorted into coated vesicles at the TGN. Sorting is believed to be mediated by the adaptor protein complex (AP-3) that interacts with dileucine, targeting motifs located in the cytoplasmic COOH-terminal tails of these proteins (Vijayasaradhi et al., 1995; Honing et al., 1998; Calvo et al., 1999). Vesicles are then transported to spherical vacuoles, termed stage I melanosomes, which resemble late endosomes at the molecular level. Stage I structures contain proteinaceous material, incomplete lamellae, and small vesicles which mature to form elliptical (eumelanosomes containing black pigment) or spherical (pheomelanosomes containing yellow pigment) stage II melanosomes in which lamellae have a more organized appearance. Stage III melanosomes are electron dense due to melanin deposition, a process which eventually results in the amorphous appearance of stage IV melanosomes. Recent elegant time-lapse microscopic experiments indicate that mammalian melanosomes undergo long range, bidirectional, microtubule-based transport and are retained or captured in peripheral dendrites by interaction with the actin cytoskeleton via the unconventional myosin, myosinVa (Wu et al., 1998; Rogers and Gelfand, 2000). Transport to and retention of melanosomes at the tips of dendrites is essential for their transfer to keratinocytes and hence normal pigmentation.

We found recently that a mouse model of HPS, *gunmetal* (*gm*), is caused by a splice site mutation in the Rab geranylgeranyl transferase (RGGT) α subunit (Detter et al., 2000). This mutation impairs the synthesis of the heterodimeric RGGT enzyme and results in 80% reduction of its activity. Surprisingly, the reduction in RGGT activity apparently leads to hypoprenylation/dysfunction of selected Rabs in selected tissues, instead of a generalized defect. In platelets, we found that Rab27 is one such Rab, suggesting that it may play an important role in both the hemorrhagic disease and the coat color dilution observed in *gm* mice (Detter et al., 2000). This observation, together with previous demonstration of high expression of Rab27 in pigmented cells (Seabra et al., 1995; Chen et al., 1997), led us to study the function of Rab27 in skin melanocytes. In the present study, we show that Rab27a is present in melanosomes and we suggest that Rab27a might act to promote peripheral retention of melanosomes via recruitment of myosinVa.

Materials and Methods

Plasmid Constructs

The cDNA encoding rat Rab27a (Seabra et al., 1995) and canine Rab1a (Seabra et al., 1992) served as template to generate the dominant negative mutants Rab27aT23N, Rab27aN133I, and Rab1aN124I, respectively, by PCR site-directed mutagenesis. These constructs, as well as human Rab5a (Farnsworth et al., 1994), were subcloned into the pEGFP-C3 vector (CLONTECH Laboratories, Inc.) and designated pEGFP-Rab27a, pEGFP-Rab27aT23N, pEGFP-Rab27aN133I, pEGFP-Rab1a, pEGFP-Rab1aN124I, and pEGFP-Rab5. The resulting plasmids encode fusion proteins that contain each Rab protein and mutant attached to the COOH terminus of the enhanced green fluorescent protein (EGFP).

Cell Culture and Transfection

Melanocyte cell lines, melan-a originated from a black mouse (Bennett et al., 1987), melan-b from a brown mouse, melan-c from an albino mouse (Bennett et al., 1989), and the human malignant melanoma cell line MM96 were kindly provided by Dorothy Bennett, St. George's Hospital Medical School, London, UK. The S91/Cloudman melanoma cell line derived from dilute mouse was obtained from the ECACC. Melan-a, melan-b, and melan-c cells were cultured in RPMI 1640 supplemented with 10% fetal calf serum, 2 mM glutamine, 0.1 mM 2-mercaptoethanol, 200 nM PMA (Calbiochem), 100 U/ml penicillin G, and 100 U/ml streptomycin at 37°C with 10% CO_2. MM96 cells were cultured in DME supplemented with 10% fetal calf serum, 2 mM glutamine, 100 U/ml penicillin G, and 100 U/ml streptomycin at 37°C with 5% CO_2. S91/Cloudman melanoma cells were cultured in Ham's F-10 medium supplemented with 10% fetal calf serum, 5% horse serum, 2 mM glutamine, 100 U/ml penicillin G, and 100 U/ml streptomycin at 37°C with 5% CO_2. Cells for immunofluorescence were grown on coverslips for 24 h, transfected using the liposomal transfection reagent Fugene 6 (Roche) and then fixed 48 h later.

To derive primary cultures, skins from neonatal *ashen* mice (1–3-d-old) were incubated with 5 ml of bovine trypsin (5 mg/ml in PBSA) for 1 h at 37°C. The epidermis was then peeled from the dermis using forceps, washed in PBSA, and cut into smaller fragments using a scalpel blade. Epidermis fragments from each mouse were then placed in 5 ml of medium (described below) containing 5 μg/ml soybean trypsin inhibitor. This mixture was then aspirated through the nozzle of a 5-ml combitip and the resulting cell suspension was plated onto a 20% confluent layer of mitomycin C–treated Xb2 murine keratinocyte derived feeder cells. Pigmented melanocytes were apparent 10–14 d after plating. Primary cultures of mu-

[1]*Abbreviations used in this paper:* CHM, choroideremia; EGFP, enhanced green fluorescent protein; *gm*, *gunmetal*; HPS, Hermansky-Pudlak syndrome; LAMP, lysosome-associated membrane protein; REP, Rab escort protein; RGGT, Rab geranylgeranyl transferase; TRP-1, tyrosinase-related protein 1.

rine melanocytes were maintained in RPMI 1640 supplemented with 5% fetal calf serum, 2 mM glutamine, 200 nM PMA, 200 pM cholera toxin (Calbiochem), 100 U/ml penicillin G, and 100 U/ml streptomycin at 37°C with 10% CO_2.

Antibodies

Antibodies Q142 and N688 are polyclonal rabbit antibodies directed against purified human His_6-Rab27a (Tolmachova et al., 1999) and rat His_6-Rab27a, respectively. His_6-Rab27a, expressed using pET14b vector, was produced in *Escherichia coli* as described previously (Seabra et al., 1995). Rabbits were immunized with 150 μg of purified His_6-Rab27a and immune bleeds were collected as described previously (Seabra et al., 1991). Anti-Rab27a antibodies were affinity purified from serum using the respective antigen cross-linked to AminoLink coupling gel (Pierce and Warriner), as described previously (Seabra et al., 1995). Q142 was used at 1:100 dilution for immunofluorescence and 1:1,000 dilution for immunoblotting. Anti-Rab27a mouse monoclonal antibody 4B12 directed against rat His_6-Rab27a was produced as described (Herz et al., 1990) and used at 1 μg/ml for immunoblotting. Other antibodies were used at the following dilutions: monoclonal antibodies Mel-5 clone Ta99 anti–TRP-1 antibody (ID Labs) (1:50) and HMB-45 (Dako) reactive against melanosome-resident protein silver/Pmel17/gp100 (1:50); polyclonal antibodies anticalnexin (1:10,000), anti-Rab5 (both StressGen Biotechnologies) (1:1,000), anti-Rab6 (Autogenbioclear) (1:500), anti-Rab8 (Transduction Laboratories) (1:1,000), antityrosinase (1:1,000) (-PEP7 generously provided by Dr. V. Hearing, National Institutes of Health, Bethesda, MD), antitransferrin receptor (1:1,000 for immunoblotting and 1:100 for immunofluorescence; Zymed Laboratories), and antimyosinVa, generously provided by C. Lionne and J. Kendrick-Jones (Medical Reasearch Council Laboratory for Molecular Biology, Cambridge, UK; 1:5,000 for immunoblotting and 1:100 for immunofluorescence). Anti-Rab escort protein (REP)1 J905 (Shen and Seabra, 1996) and anti-Rab27a N688 polyclonal antibodies were used for immunoprecipitation.

Immunoblotting and Immunofluorescence

For immunoblot analysis, samples were subjected to SDS-PAGE and transferred to polyvinyldifluoride membranes. Membranes were incubated with primary antibody diluted in solution 1 (PBS, 0.2% Tween 20, 5% nonfat dry milk) for 1 h, washed with solution 2 (PBS, 0.2% Tween 20), followed by incubation for 30 min with 1:10,000 dilution of appropriate HRP-conjugated secondary antibody (Dako) diluted in solution 1 and washing as before. Bound antibody was detected using the ECL system (Amersham Pharmacia Biotech). Blots were calibrated with prestained molecular weight standards (Bio-Rad Laboratories). For immunofluorescence, coverslip-grown cells were washed in PBS and then fixed in 3% paraformaldehyde in PBS for 15 min. Excess fixative was removed by extensive washing in PBS and quenched by incubation in 50 mM NH_4Cl for 10 min. Fixed cells were then incubated with primary antibody diluted in solution 3 (PBS, 0.5% BSA, 0.05% saponin) for 30 min, washed extensively in solution 3, and incubated for 30 min with appropriate Alexa 488– and/or Alexa 568–conjugated secondary antibodies (Molecular Probes) diluted in solution 3. Coverslips containing fixed cells were washed as before in solution 3, mounted in Immuno Fluor medium (ICN Biomedicals), and observed using a Leica DM-IRBE confocal microscope. Images were processed using Leica TCS-NT software associated with the microscope and Adobe Photoshop® 4.0 software. All images presented are single sections in the z-plane. For simultaneous immunofluorescence using two rabbit polyclonal antibodies, fixed cells stained with anti-Rab27a–reactive antibodies were paraformaldehyde fixed for a time after incubation with Alexa 488–conjugated secondary antibodies. Cells were then incubated with antimyosinVa antibodies before washing, incubation with Alexa 568–conjugated anti–rabbit antibodies, and mounting as before. To evaluate pigment distribution after overexpression of Rab27a, the area of the cytoplasm occupied by pigment granules was compared with the total area of the cytoplasm. Cells in which the area occupied by 90% of the granules was ≤50% of the total were defined as "aggregated" in Table I.

Electron Microscopy

For ultrathin section preparations, melan-a melanocytes were loaded with fluid phase HRP at 37°C for 60 min. Compartments of the endocytic pathway were then cross-linked with DAB and H_2O_2 and the cells were permeabilized with digitonin, all as described previously (Gibson et al., 1998). The cells were labeled for Rab27a with antibody Q142 (1:50), which was detected using a 10-nm gold-conjugated secondary antibody. Finally, cells were fixed in 2% paraformaldehyde/1.5% gluteraldehyde, embedded in Epon, and prepared for thin section electron microscopy.

For whole mount preparations, melan-a and *ashen* melanocytes were loaded with fluid phase HRP and cross-linked as described above. Cells were permeabilized with 1% Triton X-100 as described previously (Gibson et al., 1998) and labeled for myosinVa with the rabbit polyclonal primary antibody (1:40) and a 15-nm gold-conjugated secondary antibody and Rab27a with the mouse monoclonal 4B12 antibody (1:40) detected with a 10-nm gold-conjugated secondary antibody. Cells were fixed with 4% gluteraldehyde, osmicated, and critical-point dried. Samples were then rotary-shadowed and carbon-coated and sections were placed on grids for subsequent electron microscopy.

Table I. Overexpression of Dominant Interfering Mutants of Rab27a in Melan-a Cells Induces Aggregation of Melanosomes Close to the Nucleus

Transfected DNA	Percent dispersed	Percent aggregated
pEGFPRab27a	100	0
pEGFPRab27aT23N	87	13
pEGFPRab27aN133I	19	81
pEGFPRab1aN124I	100	0

$n = 100$.

Subcellular Fractionation

Cultured melanocytes were washed twice with 10 mM Tris-HCl, pH 7.5, 150 mM NaCl, 5 mM $MgCl^2$ and scraped in the same buffer containing 10 g/ml of aprotinin, leupeptin, pepstatin, 0.5 mM PMSF, and 1 mM DTT. Cells were homogenized in buffer containing 10 mM Hepes, pH 7.2, 1 mM EDTA, 0.25 M sucrose and protease inhibitors, by five passages through a cell cracker (EMBL). Nuclei were pelleted by centrifugation at 100 *g* for 10 min before the postnuclear supernatant was fractionated using a Percoll gradient as described previously (Orlow et al., 1993). In brief, the postnuclear supernatant was mixed with 90% Percoll in 0.25 M sucrose buffer to a final concentration of 28% Percoll and the mixture was centrifuged in a Vti 65.2 rotor (Beckman Coulter) for 48 min at 10,000 *g* at 4°C. Fractions (250 μl) were collected from the top of the gradient and centrifuged for 60 min at 100,000 *g* to remove Percoll before gel electrophoresis.

Immunoprecipitation

Melan-a and melan-b cells grown on 15-cm dishes to 80% confluency were washed three times with cold PBS, scraped, and harvested by centrifugation. Cell pellets or eye tissue, after removal of the lens from C57Bl6/J mice, were then lyzed in buffer containing 20 mM Tris-HCl, pH 7.5, 50 mM NaCl, 1 mM EGTA, 1% CHAPS, 10 μg/ml each of aprotinin, leupeptin, and pepstatin, and 0.5 mM PMSF. Lysates were centrifuged at 10,000 *g* for 15 min and the supernatant was then incubated with polyclonal antibodies (1 μg) previously immobilized on protein A–Sepharose. After overnight incubation at 4°C, the beads were precipitated by low speed centrifugation, washed four times with the same buffer, and boiled in SDS sample buffer. Precipitated proteins were separated on 4–15% gradient SDS polyacrylamide gel, transferred to polyvinyldifluoride membrane, and immunoblotted as described above.

Online Supplemental Material

Online supplemental materials can be found at http://www.jcb.org/cgi/content/full/152/4/795/DC1.

Figure S1 shows low power images of fields of melan-c melanocytes labeled with anti-Rab27a antibodies taken using a 203 objective lens. It shows that Rab27a was typically distributed in 0.5-mm-diameter structures located in the peripheral cytoplasm and dendrites, which contain TRP-1 and silver protein, as well as diffuse cloudy pattern close to the nucleus.

In Figure S2, to ensure the specificity of binding of the Alexa 568–conjugated goat anti–rabbit secondary antibody used to detect antimyosinVa in Fig. 6, we incubated melan-c cells already stained for Rab27a using polyclonal antibodies (detected using Alexa 488–conjugated goat anti–rabbit secondary antibodies) with Alexa 568–conjugated goat anti–rabbit secondary antibody alone. We found that almost no Alexa 568–conjugated goat anti–rabbit secondary antibody bound to cells in the absence of the antimyosinVa polyclonal antibody (Figure S2 E).

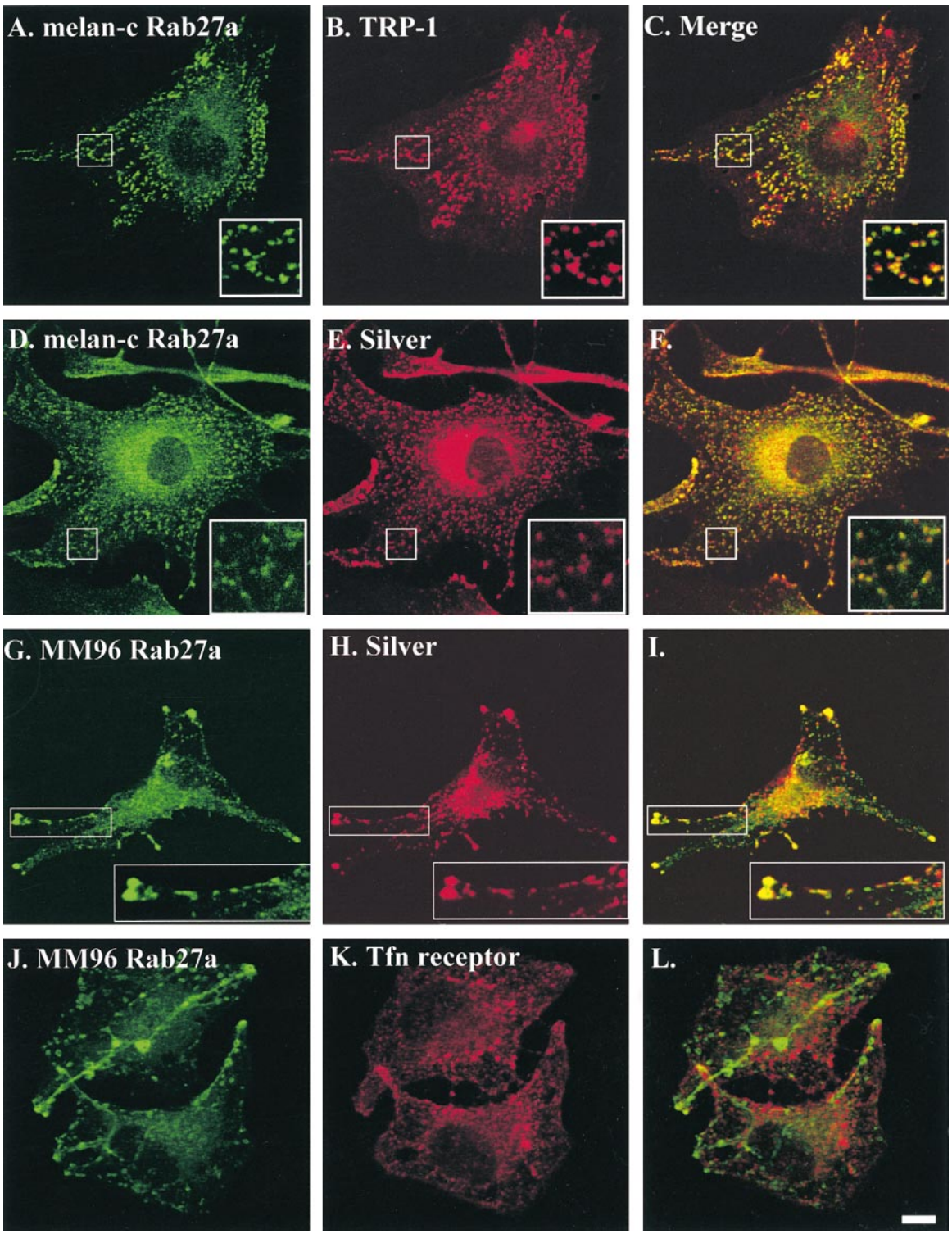

Figure 1. Rab27a colocalizes with melanosome-resident proteins in MM96 and melan-c cells. Coverslip-grown melan-c or MM96 cells were fixed and stained using the polyclonal anti-Rab27a antibody Q142 (A, D, G, and J); monoclonal antibodies reactive to the melanosomal marker proteins TRP-1 (B) or silver (E and H); and the transferrin receptor (Tfn; panel K), an endosome marker, as described in Materials and Methods. Polyclonal antibodies were detected using Alexa 488–conjugated goat anti–rabbit secondary antibodies (A, D, G, and J); monoclonal antibodies were detected using Alexa 568–conjugated goat anti–mouse second antibodies (B, E, H, and K). Merged fluorescent signals for Rab27a and the indicated marker proteins are shown in C, F, I, and L. Bar, 10 μm. See Figure S1, available at http://www.jcb.org/cgi/content/full/152/4/795/DC1.

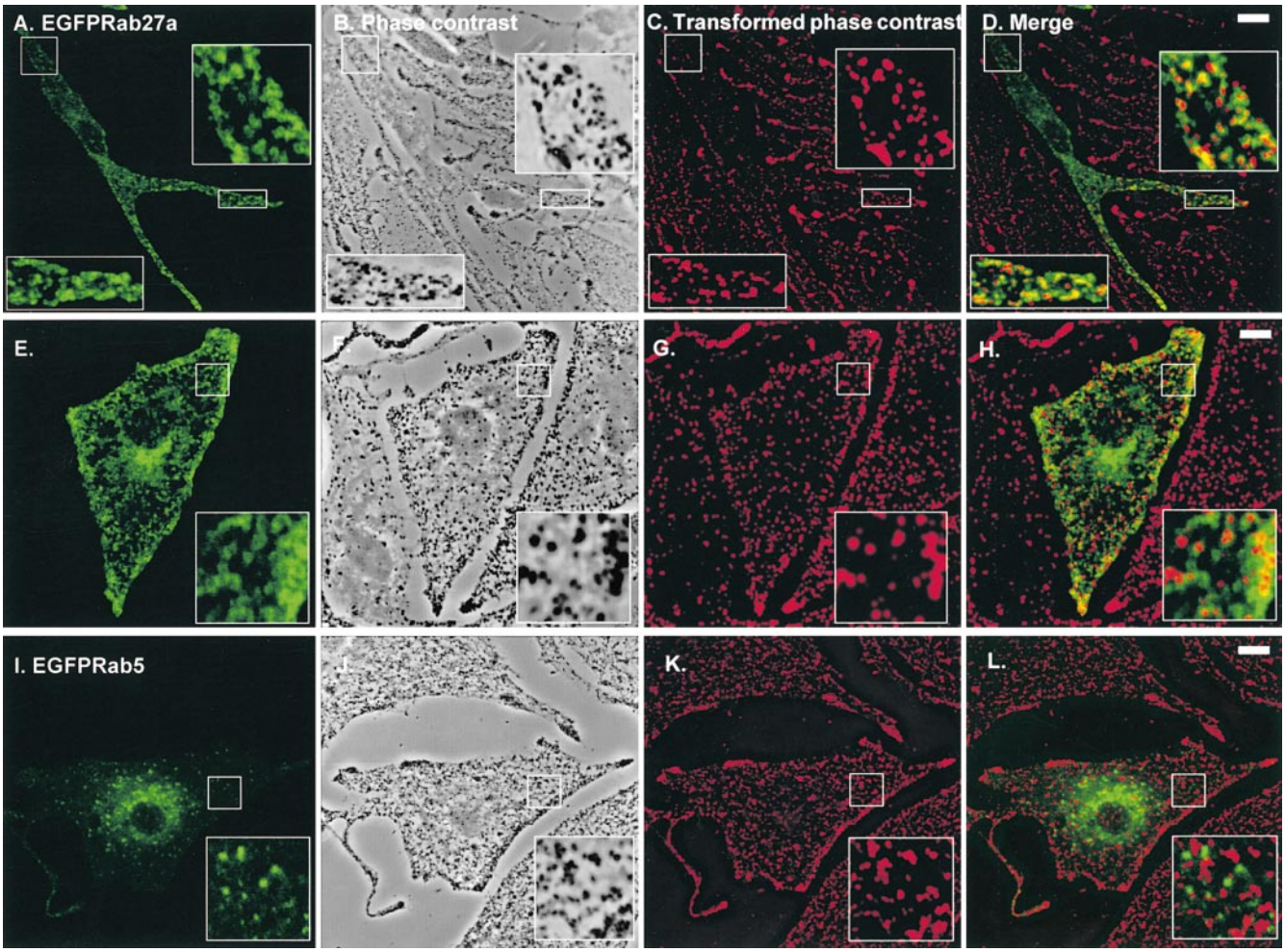

Figure 2. Transiently overexpressed EGFP-Rab27a is associated with pigment granules in melan-a cells. Melan-a cells were transfected with pEGFP-Rab27a (A–H) or pEGFP-Rab5 (I–L) and fixed 48 h later, as described in Materials and Methods with the following modification. After transfection, cells were permeabilized for 5 min before fixation in solution 4 (80 mM K-Pipes, pH 6.8, 5 mM EGTA, 1 mM $MgCl_2$, 0.05% saponin) in order to remove nonmembrane-associated fusion protein. A, E, and I show the distribution of the indicated overexpressed EGFP-Rab fusion protein in melan-a cells. B, F, and J are phase–contrast images of melan-a cells showing the distribution of pigment granules in transfected cells. Phase–contrast images (B, F, and J) of melan-a cells were transformed into pseudocolor (red) images, shown in C, G, and K, using Adobe Photoshop® 4.0 and then merged with the green fluorescence signal emitted by overexpressed EGFP-Rab27a or EGFP-Rab5 proteins, respectively (D, H, and L). Bars, 10 μm.

Results

Colocalization of Rab27a with Melanosomes

We first confirmed that Rab27a protein is highly expressed in melanocytes. We immunoblotted detergent lysates of several cultured cell lines using an affinity-purified rabbit polyclonal anti–human Rab27a antibody, Q142. This antibody was highly specific for Rab27a and did not cross-react with Rab27b or any other Rab proteins tested (data not shown). We observed high levels of Rab27a expression in nonpigmented melanocytic cell lines, melan-c and MM96, lower levels of Rab27a expression in pigmented cell lines, melan-a and melan-b, and only very low levels of expression of Rab27a in several different cultured fibroblast cell lines (data not shown). These data are consistent with an earlier report of the expression of the Rab27a mRNA and demonstrate the specificity of the anti-Rab27a antibody (Chen et al., 1997).

The finding that Rab27a is highly expressed in melanocyte and melanoma-derived cells suggested that Rab27a might be associated with a transport pathway or organelles specific to melanocytes. We then examined the subcellular localization of the protein by immunofluorescence microscopy in nonpigmented melan-c melanocytes, derived from an albino mouse that lacks tyrosinase activity, and the human melanoma–derived cell line MM96 (Fig. 1). In melan-c and MM96 cells, the Q142 antibody revealed that Rab27a primarily localizes to peripheral organelles (~0.5 μm in diameter) (Fig. 1, A, D, G, and J). In most cases, peripheral Rab27a-positive structures also contained melanosome-resident proteins: TRP-1 (Fig. 1, A–C) and silver protein/Pmel17/gp100 (HMB-45) (Fig. 1, D–I). Electron microscopy indicated that these structures are melanosomes, as they contained a fibrillar core but lacked melanin (data not shown). In MM96 cells, we observed a similar pattern. Rab27a is distributed on linear structures extending from

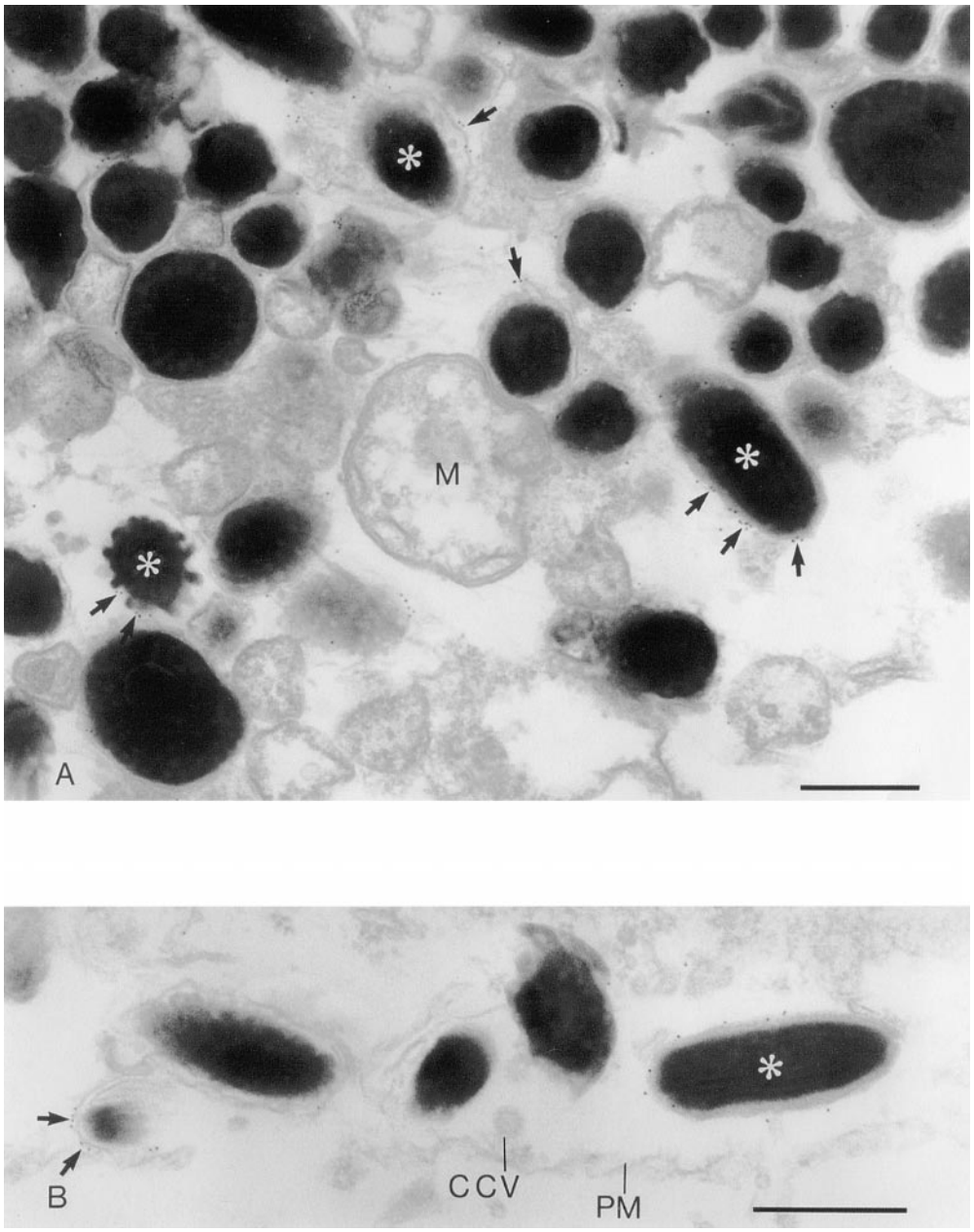

Figure 3. Immunoelectron microscopy of Rab27a in melan-a cells. (A) Melan-a melanocytes contain predominantly stage IV melanosomes, many of which are labeled for Rab27a. Melan-a melanocytes were permeabilized with digitonin and the anti-Rab27a antibody detected with a 10-nm gold-conjugated secondary antibody as described in Materials and Methods. The presence of representative gold particles is indicated by arrows. Mitochondria (M) are demonstrative of other organelles in the melanocyte that show a very low level of background labeling. (B) Rab27a-positive melanosomes lie just below the plasma membrane (PM) adjacent to a clathrin-coated vesicle (CCV). Bars, 0.5 μm.

the cell body into the peripheral dendrites (Fig. 1 J). We also observed partial colocalization of Rab27a with the lysosome-resident LAMP-1 (data not shown), which also associates with melanosomes (Orlow et al., 1993). In many cells we observed a diffuse, cloudy pattern Rab27a staining close to the nucleus (Fig. 1, D and G). This pattern could correspond to small Rab27a-containing membrane vesicles rather than cytosolic protein, as immunoblotting of S100 fractions prepared from the same cells were devoid of Rab27a (data not shown). Staining of these cells with antibodies reactive to proteins resident in other compartments of the secretory and endocytic pathways (Fig. 1, J–L, and data not shown) suggests that little Rab27a associates with another identifiable membrane-bound organelle.

We next sought to extend these observations by transient overexpression of EGFP-Rab27a fusion protein. Previous reports indicate that attachment of EGFP to the NH_2 terminus of other Rab proteins does not affect targeting of the resulting EGFP-tagged Rab proteins relative to their nontagged counterparts (Roberts et al., 1999; White et al., 1999). We observed that EGFP-Rab27a fusion protein was distributed mainly in the periphery of pigmented melan-a (Figs. 2, A–H) and melan-b (data not shown) cells forming ring-like patterns. Close examination indicates that many of the rings of EGFP-Rab27a appear to surround pigment granules, suggesting that Rab27a decorates the cytoplasmic surface of granules. We also observed significant colocalization of overexpressed Rab27a fusions with the melanosome-resident protein tyrosinase in melan-b cells (data not shown). In contrast, overexpressed EGFP-Rab5 (Fig. 2, I–L), EGFP-Rab1, EGFP-Rab6, and EGFP-Rab8 (data not shown) fusion proteins did not colocalize with melanosomes in these cell lines, indicating the specificity of the association of the EGFP-Rab27a fusion protein with me-

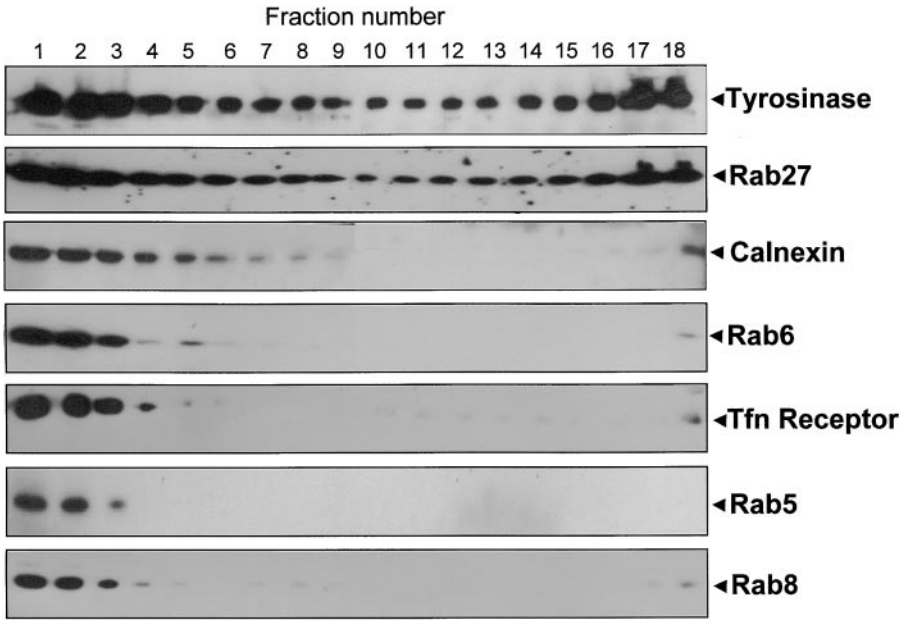

Figure 4. Subcellular fractionation of melanocyte-derived membranes. Postnuclear supernatants of melan-a cells were subjected to a 28% Percoll gradient centrifugation; fractions were then collected from the top of the gradient and analyzed by immunoblot. The lightest fraction is 1 (top of the gradient) and the densest fraction is 18 (bottom of the gradient). Antibodies used are indicated on the right. Rab5, Rab6, and Rab8 localize to early endosomes, Golgi, and TGN/plasma membrane, respectively. Calnexin, the transferrin (Tfn) receptor, and tyrosinase are membrane proteins that localize to the ER, early endosomes, and melanosomes, respectively.

lanosomes. Together these results suggest that endogenous and overexpressed Rab27a protein may be associated with the limiting membrane of melanosomes.

To substantiate light microscopic observations, we then used immunoelectron microscopy to examine the localization of endogenous Rab27a in melan-a cells, which contain mostly late stage melanosomes. Cells were permeabilized to give access to the cytoplasmic face of the perimeter membrane of the organelles and then incubated with anti-Rab27a antibody. As shown in Fig. 3, Rab27a labeled melanosomes, most of which were late stage structures (i.e., stage IV), as indicated by their electron-dense appearance and ellipsoid shape. The gold label appeared to be distributed over the surface of the limiting membrane of melanosomes, as indicated in Fig. 3 B. Labeled melanosomes were often distributed in the vicinity of the plasma membrane, whereas other membrane-bound organelles, such as lysosomes and multivesicular endosomes, were unlabeled.

Subcellular Fractionation Confirms the Association of Rab27a with Melanosomes

To confirm our morphological observations, we subjected melan-a cellular membranes to ultracentrifugation in a Percoll gradient under conditions which separate melanosomes from other cellular membranes due to their high density (Orlow et al., 1993). Immunoblotting of gradient fractions revealed that most Rab27a is present in two peaks (Fig. 4). One peak (fractions 15–18) corresponded to relatively dense membrane fractions, which contained a significant amount of tyrosinase and melanin, but not calnexin (a marker of the ER), Rab6 (a marker of Golgi vesicles), transferrin receptor and Rab5 (markers of endosomes), or Rab8 (a marker of post-Golgi vesicles) (Fig. 4). The lighter (earlier) fractions seem to include most of the other cellular membranes as they contained calnexin, Rab6, transferrin receptor, Rab5, and Rab8. In summary, subcellular fractionation confirms the presence of Rab27a on melanosomes.

Overexpression of Dominant Negative Rab27a Mutants Causes Alteration in the Distribution of Melanosomes in Cultured Melanocytes

To address the function of Rab27a in cultured melanocytes, we attempted to disrupt its function by transient overexpression of Rab27a mutants, Rab27aT23N and N133I, equivalent to the dominant interfering RasS17N and N116I mutants, respectively. Transient overexpression of many other Rabs containing corresponding changes has been shown to specifically disrupt the function of the endogenous protein (e.g., Walworth et al., 1989). The RasS17N and N116I mutants bind to guanine nucleotide exchange factors with higher affinity than wild-type Ras, thereby preventing activation of the wild-type protein (Feig, 1999). The Rab mutants are believed to act similarly.

Transient overexpression experiments revealed that EGFP-Rab27aT23N and EGFP-Rab27aN133I fusion proteins were predominantly cytosolic and that their expression (Fig. 5, E–L), but not the wild-type (Figs. 2, A–H and 5, A and B) or the constitutively active mutant Rab27aQ78L (not shown), resulted in dramatic redistribution of pigment granules in melan-a cells. In cells expressing either of the dominant interfering mutants, pigment granules are observed to cluster close to the nucleus (Fig. 5, E–L) in contrast to nontransfected cells and those transfected with wild-type EGFP-Rab27a in which pigment granules are distributed evenly throughout the cytoplasm (Figs. 2, B and F, and 5 B). Similar effects on granule positioning were induced by overexpression of nontagged and myc-tagged Rab27aT23N and Rab27aN133I mutants, and with another pigmented cell line, melan-b (data not shown). We also found that the Rab27aT23N and Rab27aN133I mutants differ in their ability to cause perinuclear clustering of melanosomes, their expression resulting in this phenomenon in 13 and 81% of transfectants, respectively (Table I). This result corresponds with previous studies suggesting that the Ras-equivalent N116I mutant elicits a stronger dominant negative effect than the S17N mutant, as we could not detect significant differ-

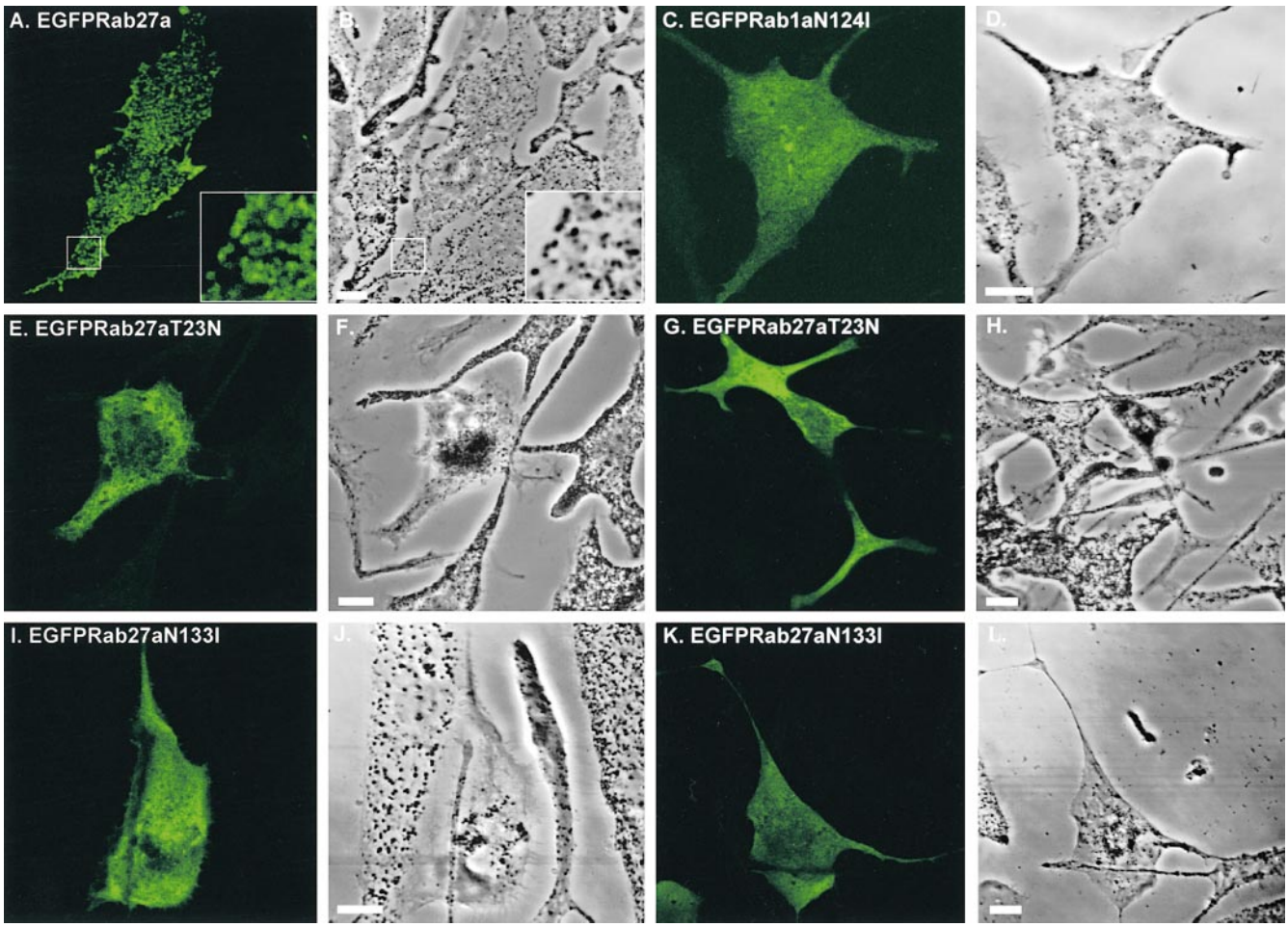

Figure 5. Transient overexpression of dominant interfering Rab27a mutants, Rab27aT23N and Rab27aN133I, results in perinuclear clustering of pigment granules in melanocytes. Melan-a cells were transfected with pEGFP-Rab27a (A and B), pEGFP-Rab1aN124I (C and D), pEGFP-Rab27aT23N (E–H), or pEGFP-Rab27aN133I (I–L) and fixed 48 h later, as described in Materials and Methods. A, C, E, G, I, and K show the distribution of the indicated overexpressed EGFP-Rab fusion protein in melan-a cells. B, D, F, H, J, and L are phase–contrast images showing the distribution of pigment granules in these cells. Bars, 10 μm.

ences between the levels of mutant protein expressed (Tisdale et al., 1992). We never observed this effect in wild-type Rab27a transfected cells or in cells transfected with EGFP-Rab1, EGFP-Rab1aN124I (Fig. 5, G and H), EGFP-Rab5 (Fig. 2, I–L), EGFP-Rab6, or EGFP-Rab8 (data not shown).

Interestingly, the distribution of pigment granules in melanocytes overexpressing Rab27a dominant negative mutants is very similar to that observed after expression of dominant negative myosinVa constructs (Wu et al., 1998). Furthermore, the results of recent studies suggest that myosinVa participates in the retention of melanosomes in the periphery of melanocytes (for review see Rogers and Gelfand, 2000), suggesting that Rab27a and myosinVa cooperate in establishing and/or maintaining the peripheral distribution of melanosomes in melanocytes. The finding that a proportion of myosinVa is present on melanosomes in melanocytes also supports this idea (Nascimento et al., 1997; Wu et al., 1997).

Rab27a Colocalizes with Melanosome-associated MyosinVa

To test the possible functional interaction of melanosome-associated Rab27a and myosinVa, we investigated whether the two proteins exhibit similar patterns of intracellular distribution. We did this using two approaches.

First, we employed immunofluorescence microscopy to examine the extent of colocalization of endogenous myosinVa with either transiently overexpressed EGFP-Rab27a or endogenous Rab27a in nonpigmented melan-c and MM96 cells (Fig. 6 and data not shown). We observed a high level of coincidence in the distribution of both overexpressed and endogenous Rab27a with endogenous myosinVa in melan-c and MM96 cells (Fig. 6 and data not shown). Cytoplasmic structures (0.5-μm diameter) containing Rab27a and myosinVa were defined as melanosomes by staining with anti–TRP-1 antibodies (data not shown). The subcellular distribution of Rab27a in these cells appears to coincide more closely with that of myosinVa than with that of the melanosome-resident proteins examined above (compare Fig. 6 with Figs. 1 and 2). Interestingly, immunoblotting revealed that nonpigmented cells, melan-c and MM96, express higher levels of myosinVa relative to the pigmented melanocytes melan-a and melan-b, as found for Rab27a (data not shown).

To examine more precisely the proximity of endogenous melanosome-associated Rab27a and myosinVa, we performed double immunoelectron microscopy of melan-a cells using ultrathin and whole mount preparations (Fig. 7). Clusters of Rab27a (10-nm gold) and myosinVa (15-nm

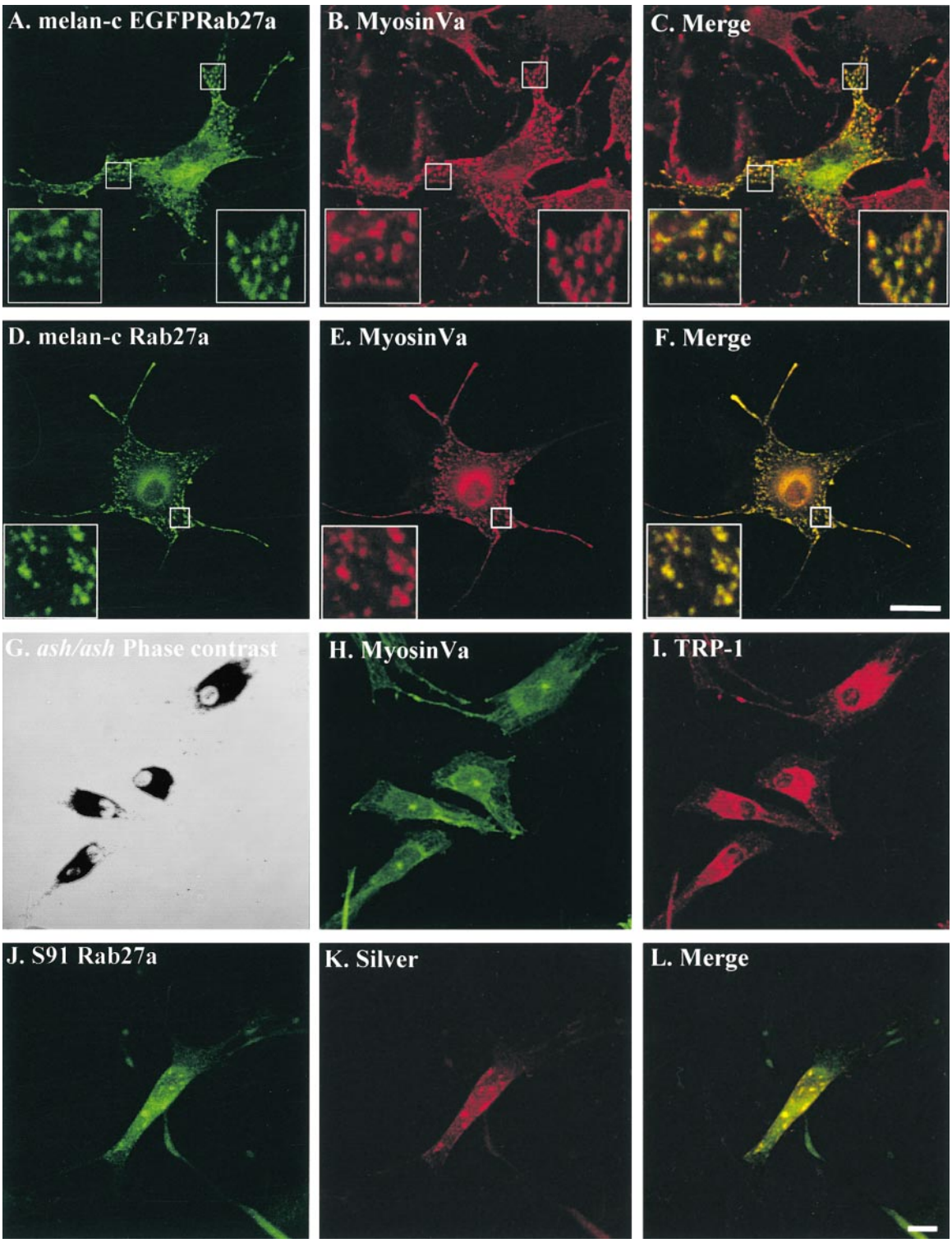

Figure 6. MyosinVa colocalizes with Rab27a on melanosomes in wild-type melanocytes, but is absent from melanosomes in Rab27a mutant *ashen* melanocytes. (A–F) Melan-c cells were transfected with pEGFP-Rab27a (A) and fixed 48 h later. Endogenous Rab27a in fixed melan-c cells was stained using the polyclonal anti-Rab27a antibody Q142 detected using Alexa 488–conjugated goat anti–rabbit antibodies (D). Residual bound anti-Rab27a antibody, not detected by the Alexa 488–conjugated goat anti–rabbit antibodies, was then destroyed by a second round of fixation (see Materials and Methods). Transfected or anti-Rab27a–stained cells were then stained for myosinVa using polyclonal antimyosinVa antibody detected using Alexa 568–conjugated goat anti–rabbit antibodies (B and E). (G–I) Coverslip-grown primary cultures of melanocytes derived from the murine Rab27a mutant *ashen* were fixed and stained with antimyosinVa polyclonal antibodies and anti–TRP-1 monoclonal antibodies which were detected using Alexa 488–conjugated goat anti–rabbit antibodies (H) and Alexa 568–conjugated goat anti–mouse antibodies (I). G is a phase–contrast image showing the perinuclear distribution of melanosomes in *ashen* melanocytes. (J–L) Coverslip-grown S91/Cloudman melanoma cells derived from the murine myosinVa mutant *dilute* were fixed and stained with polyclonal anti-Rab27a antibody and monoclonal HMB-45 antibody detected using Alexa 488–conjugated goat anti–rabbit antibodies (J) and Alexa 568–conjugated goat anti–mouse antibodies (K). C, F, and L show merged fluorescence images. Bars, 20 μm. See supplemetal figure S2, available at http://www.jcb.org/cgi/content/full/152/4/795/DC1.

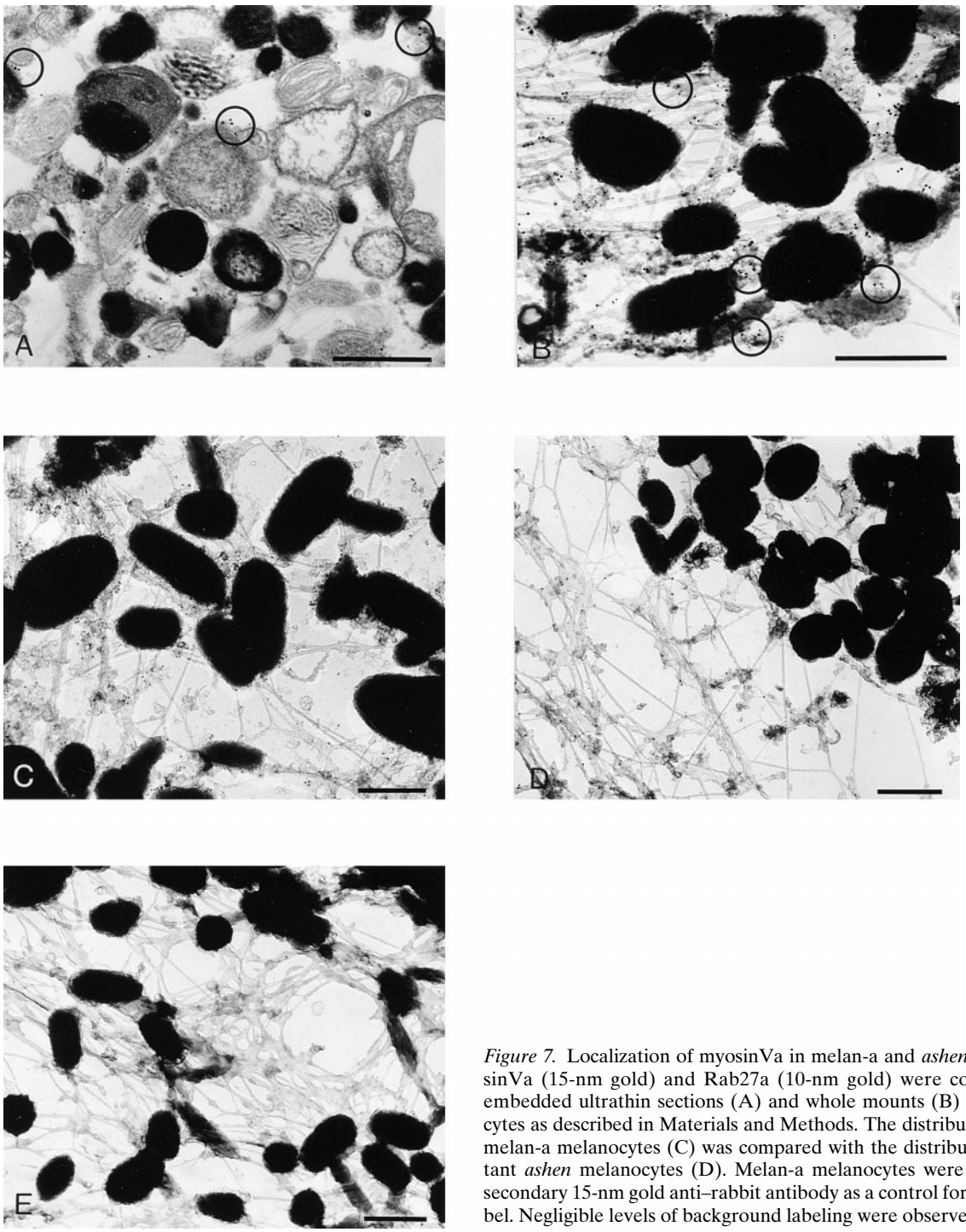

Figure 7. Localization of myosinVa in melan-a and *ashen* melanocytes. MyosinVa (15-nm gold) and Rab27a (10-nm gold) were colocalized in Epon-embedded ultrathin sections (A) and whole mounts (B) of melan-a melanocytes as described in Materials and Methods. The distribution of myosinVa in melan-a melanocytes (C) was compared with the distribution in Rab27a mutant *ashen* melanocytes (D). Melan-a melanocytes were incubated with the secondary 15-nm gold anti–rabbit antibody as a control for specificity of the label. Negligible levels of background labeling were observed (E). Bar, 0.5 μm.

gold) were observed on the perimeter membrane of melanosomes in ultrathin sections of permeabilized melan-a cells (Fig. 7 A). Whole mount preparations (Fig. 7, B and C) were made in order to gain an overview of the myosinVa content of the cell while preserving the actin cytoskeleton. MyosinVa is abundant within melan-a melanocytes and is localized on material attached to the actin cytoskeleton as well as over the surface membrane of melanosomes, often at sites in which the melanosomes and cytoskeletal filaments lie in close proximity. The whole mount confirms the partial colocalization of Rab27a and myosinVa at the cytoplasmic face of melanosomes (Fig. 7 B) and the association of these gold labels with cytoskeletal elements.

Rab27a May Be Required for the Association of MyosinVa with Melanosomes

To investigate further the possible functional interplay between Rab27a and myosinVa, we asked whether one role of Rab27a might be to mediate the association of myosinVa with melanosomes. To address this possibility, we employed immunofluorescence and immunoelectron microscopy to investigate the subcellular localization of myo-

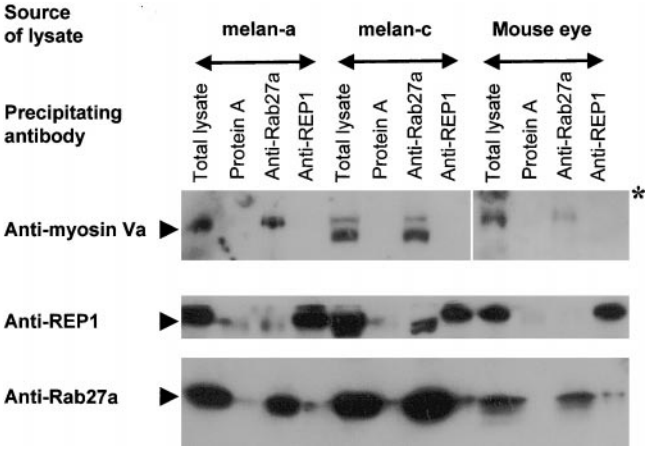

Figure 8. Coimmunoprecipitation of Rab27a and myosinVa. Melanocyte or mouse eye lysates were incubated with the indicated antibodies. The adsorbed material was precipitated and analyzed by immunoblot as described in Materials and Methods.

sinVa in primary cultures of melanocytes derived from the skins of *ashen* mutant mice. As discussed below in more detail, *ashen* mice bear a loss-of-function mutation in the Rab27a gene (Wilson et al., 2000).

We found that pigment granules in *ashen* melanocytes cluster close to the nucleus rather than being evenly distributed in peripheral cytoplasmic locations, as we observed for melan-a and melan-b melanocytes (Figs. 2 and 6 and data not shown). These observations are consistent with previous reports of the phenotype of melanocytes derived from *dilute* and *ashen* mutants (Provance et al., 1996; Wilson et al., 2000). When we stained for myosinVa, we observed that much of the myosinVa in *ashen* melanocytes is mostly excluded from the melanosome perinuclear mass. Instead, myosinVa appears concentrated in a clearly defined spot, which appears to coincide with the microtubule organizing center, as indicated by costaining with anti–α-tubulin antibodies, and the remainder is distributed throughout the cytoplasm (Fig. 6 and data not shown). This contrasts with clear melanosome association of myosinVa in melan-a and melan-c melanocytes (Figs. 6 and 7), and in primary cultures of melanocytes derived from wild-type C3H mice (the background strain of the *ashen* mutant) in which myosinVa is abundant on melanosomes (data not shown). Staining of *ashen* melanocytes with antibodies reactive to other melanosome-resident proteins, e.g., TRP-1 (Fig. 6 I) and silver (data not shown), confirmed that the clustered pigmented structures containing little myosinVa were indeed melanosomes. Interestingly, we observe that in *ashen* melanocytes some melanosomes are present in peripheral dendrites, unlike the majority in a perinuclear cluster (Fig. 6 G). A similar distribution of melanosomes was observed in melan-a melanocytes overexpressing Rab27a dominant negative proteins (Fig. 5) and in dilute melanocytes or melanocytes expressing dominant negative mutants of myosinVa (Wu et al., 1998). These peripheral melanocytes may reach the periphery via microtubule-based transport, as suggested by Wu et al. (1998). Immunoelectron microscopy data fully confirmed the immunofluorescence observations. In comparison with the wild-type melan-a (Fig. 7 C), myosinVa was expressed at a much lower level in *ashen* melanocytes. There were concentrations of melanosomes in the perinuclear area, but these were not labeled with myosinVa. Most of the myosinVa label in these cells was associated with the actin cytoskeleton (Fig. 7 D).

These data suggest that Rab27a is required for the association of myosinVa with melanosomes in wild-type melanocytes, i.e., that Rab27a functions upstream of myosinVa. One prediction of this hypothesis is that Rab27a should be targeted to melanosomes in the absence of myosinVa. Therefore, we examined the intracellular location of Rab27a in the S91/Cloudman melanoma cell line, derived from dilute (myosinVa mutant) mice (Yasamura et al., 1966). We observed by immunofluorescence microscopy that Rab27a was present in punctate cytoplasmic structures which also contained the melanosome-resident proteins silver and LAMP-1 (Fig. 6, J–L, and data not shown). These observations further support the possibility that Rab27a recruits myosinVa to melanosomes in melanocytes.

Coimmunoprecipitation of Rab27a and MyosinVa

A second prediction of this hypothesis is that Rab27a and myosinVa interact. Therefore, we examined whether myosinVa can be precipitated from detergent extracts of cultured murine melanocytes or murine tissues using affinity-purified anti-Rab27a antibodies. We observed that myosinVa is precipitated by anti-Rab27a antibodies in extracts prepared from melan-a and melan-c cells and mouse eyes (Fig. 8), but not in those from HeLa cells or mouse brain where Rab27a is not expressed (data not shown). Precipitation of myosinVa appears specific, as it was absent from precipitates prepared using anti-REP1 antibodies or protein A beads (Fig. 8) as well as murine brain extracts in which Rab27a is undetectable (data not shown; Seabra et al., 1995; Chen et al., 1997).

Discussion

The data presented here suggest a possible function for the Rab27a GTPase in establishing and/or maintaining the peripheral distribution of melanosomes in melanocytes. Our results indicate that Rab27a protein is highly expressed in melanocytes, that Rab27a is associated with melanosomes, and that overexpression of dominant negative mutants of Rab27a causes redistribution of melanosomes from the cell periphery and perinuclear clustering of melanosomes. We also report that Rab27a and myosinVa colocalize and interact in melanocytes and that Rab27a may recruit myosinVa to melanosomes, as little myosinVa is found on melanosomes in the absence of Rab27a.

We present morphological and biochemical data consistent with the association of Rab27a with melanosome membranes (Figs. 1–4). First, Rab27a colocalizes with pigmented melanosomes in cultured melanocytes (melan-a and melan-b) by immunofluorescence and immunoelectron microscopy (Figs. 2 and 3). Second, Rab27a colocalizes with peripheral structures labeled by melanosome markers in amelanotic melanocytes (melan-c) and melanoma-derived cells (MM96) by immunofluorescence microscopy (Fig. 1). Third, Rab27a cofractionates with tyrosinase, but not other organelle markers in Percoll gradients of melanocyte membranes (Fig. 4). Rab27a ap-

pears to reside predominantly in mature melanosomes. Immunoelectron microscopy shows Rab27a to be associated predominantly with type III and type IV melanosomes, whereas the association of Rab27a with type I and II melanosomes was less evident (Fig. 3; our unpublished observations).

We also show that overexpression of two independent dominant negative mutants of Rab27a, but not Rab1a, results in clustering of melanosomes in the perinuclear area in two pigmented melanocyte cell lines (Fig. 5 and data not shown). This suggests that one aspect of Rab27a function is establishing and/or maintaining the peripheral localization of melanosomes in dendritic processes. This possibility is supported by the fact that melanosomes are clustered around the nucleus in melanocytes derived from *ashen* mice (Fig. 6; Wilson et al., 2000) and Griscelli disease patients (Bahadoran et al., 2001), both of which were recently found to contain loss-of-function mutations in the murine and human Rab27a loci, respectively (Menasche et al., 2000; Wilson et al., 2000). In contrast to the results obtained using dominant negative mutants, we did not observe enhanced dispersion of melanosomes after overexpression of wild-type Rab27a or the GTPase-deficient mutant (Rab27aQ78L) (Fig. 5 and data not shown). The vast majority of melanosomes in the cultured mammalian melanocytes used in this study are already located at the periphery and contain Rab27a and myosinVa (Figs. 1, 2, and 6). Hence, their steady-state location is unlikely be altered by overexpression of wild-type or GTPase-deficient (constitutively active) protein, as this is likely merely to enhance the interaction between myosinVa and Rab27a and further stabilize their peripheral retention. However, we note that fixed cells were used for these studies and more subtle motility effects may have been missed.

A current model for the transport of melanosomes in mouse melanocytes is based on the work of Wu et al. (1998). This model envisages that melanosomes mature in the melanocyte cell body region, undergo bidirectional transport along microtubules, which extend into the dendrites, and are then "captured" and retained in peripheral regions by interaction with the local actin cytoskeleton via myosinVa. Consistent with this hypothesis, loss of myosinVa function as observed in the mouse *MyoVa* gene mutant *dilute* or, due to overexpression of a dominant interfering myosinVa construct, results in accumulation of melanosomes in the perinuclear region of melanocytes (Mercer et al., 1991; Provance et al., 1996; Wu et al., 1998). As it is now clear that Rab27a is also a critical player in this process, one important question is, how are Rab27a and myosinVa cooperating in the peripheral capture of melanosomes?

The current results lead us to hypothesize that Rab27a recruits myosinVa to melanosomes, thus mediating their peripheral "capture." Several lines of evidence support this possibility. First, Rab27a and myosinVa colocalize to melanosomes (Figs. 6 and 7). In particular, electron microscopy indicates that myosinVa and Rab27a are not evenly distributed over the cytoplasmic surface of melanosomes, rather both are clustered together in groups whose location often coincides with that of actin filaments seen in labeled whole mount sections (Fig. 7, B and C). Second, significantly less myosinVa is associated with melanosomes in *ashen* melanocytes (Rab27a mutant) compared with wild-type melanocytes (Figs. 6 and 7). Interestingly, we observed that the association of myosinVa with the centrosome is more pronounced in *ashen* melanocytes than in other mouse melanocytes used in this study or in primary cultures derived from C3H mice (Fig. 6 and data not shown). Previous studies have reported the association of myosinVa with the centrosome via the COOH terminus globular tail of myosinVa (Espreafico et al., 1998; Tsakraklides et al., 1999). The role for centrosomal myosinVa is unclear. Nevertheless, our studies suggest that Rab27a is able to influence the distribution of a significant fraction of the myosinVa cellular pool, which becomes associated with melanosomes. Third, Rab27a can be targeted to organelles containing melanosomal markers in *dilute* cells (myosinVa mutant), indicating that Rab27a does not require functional myosinVa for targeting to melanosomes (Fig. 6). Finally, myosinVa can be coimmunoprecipitated from melanocytes and mouse tissues with anti-Rab27a antibodies, indicating that both proteins interact (Fig. 8). Precedence for such a mechanism of action for Rab27a comes from the finding that activation of other Rab proteins results in specific recruitment of "effector" proteins, which in each case are thought to mediate the function of the Rab (Stenmark et al., 1995; Guo et al., 1999; McBride et al., 1999; Allan et al., 2000).

The precise mechanism by which Rab27a recruits myosinVa to melanosomes remains to be clarified in future studies. Despite some effort, we have not yet been able to determine whether the Rab27a and myosinVa interaction is direct. However, it is possible that the interaction is indirect, as there is genetic evidence that at least one more gene product is involved in this process. Melanocytes derived from the *leaden* mutant (whose gene is unknown), like those derived from *ashen* and *dilute*, exhibit perinuclear clustering of melanosomes (Provance et al., 1996) and all three coat color phenotypes are rescued by the *dilute suppressor* mutant (Moore et al., 1988). These observations suggest that all four proteins act in the same pathway, perhaps as components of a complex containing Rab27a and myosinVa. The future isolation of the components of the proposed complex, including the products of the *dilute suppressor* and *leaden* loci, may provide important clues to the molecular mechanisms regulating organelle motility in general and melanosome motility in particular.

Rab27a has also been implicated in two other disease states involving defects in Rab lipidation and membrane association. One example is the *gm* mouse, which led to the studies presented here (Detter et al., 2000). The coat color dilution observed in *gm* may result from dysfunction of Rab27a in melanocytes, given the evidence discussed here. Another example is the X-linked human retinal degenerative disease, choroideremia (CHM) (Seabra et al., 1995). In CHM, a protein required for the posttranslational geranylgeranylation and membrane association of Rab proteins, REP1 is mutated (Seabra et al., 1992, 1993). This defect does not result in a general defect in Rab prenylation in CHM, since REP function is redundant in mammalian cells and can be compensated by REP2. For unknown reasons, Rab27a is not a good substrate for REP2 and is selectively dysfunctional in CHM cells, sug-

gesting that it may act as a trigger for the retinal degeneration (Seabra et al., 1995). In light of our present data and that of others (Menasche et al., 2000; Wilson et al., 2000), it is possible that the retinal phenotype of CHM patients may result in part from defects in melanosome transport in the retinal pigmented epithelium and choroid. However, it is likely that dysfunction of other Rabs may contribute to this phenotype.

This work strengthens the idea that Rabs could be important regulators of membrane–cytoskeleton interactions. The regulation of membrane motility may indeed be a general role for Rabs, in addition to their more established role in transport vesicle docking. Future work should be directed towards a more detailed molecular description of Rab27a function in melanocytes.

We thank Janmeet Anant and Jose Ramalho for making the Rab27 mutants; Bruno Goud and Sharon Tooze laboratories for technical help; William Gahl, Dorothy Bennett, Vincent Hearing, Corinne Lionne, and John Kendrick-Jones for the generous gift of reagents; Robert Ballotti for sharing information on Griscelli patient melanocytes before publication; and Dorothy Bennett, Elena Svideskaya, and Simon Hill for helpful discussions and help with primary culture of murine melanocytes.

This work was supported by the Wellcome Trust, the Medical Research Council, the Human Frontier of Science Program, and the Foundation Fighting Blindness.

Submitted: 17 August 2000
Revised: 20 November 2000
Accepted: 22 November 2000

References

Allan, B.B., B.D. Moyer, and W.E. Balch. 2000. Rab1 recruitment of p115 into a cis-SNARE complex: programming budding COPII vesicles for fusion. *Science*. 289:444–448.

Bahadoran, P., E. Aberdam, F. Mantoux, R. Busca, K. Bille, N. Yalman, G. de Saint-Basile, R. Casaroli-Marano, J.-P. Ortonne, R. Ballotti. 2001. Rab27a: a key to melanosome transport in human melanocytes. *J. Cell Biol.* 152:843–849.

Bennett, D.C., P.J. Cooper, and I.R. Hart. 1987. A line of non-tumorigenic mouse melanocytes, syngeneic with the B16 melanoma and requiring a tumour promoter for growth. *Int. J. Cancer.* 39:414–418.

Bennett, D.C., P.J. Cooper, T.J. Dexter, L.M. Devlin, J. Heasman, and B. Nester. 1989. Cloned mouse melanocyte lines carrying the germline mutations albino and brown: complementation in culture. *Development*. 105:379–385.

Calvo, P.A., D.W. Frank, B.M. Bieler, J.F. Berson, and M.S. Marks. 1999. A cytoplasmic sequence in human tyrosinase defines a second class of di-leucine-based sorting signals for late endosomal and lysosomal delivery. *J. Biol. Chem.* 274:12780–12789.

Chavrier, P., and B. Goud. 1999. The role of ARF and Rab GTPases in membrane transport. *Curr. Opin. Cell Biol*. 11:466–475.

Chen, D., J. Guo, T. Miki, M. Tachibana, and W.A. Gahl. 1997. Molecular cloning and characterization of rab27a and rab27b, novel human rab proteins shared by melanocytes and platelets. *Biochem. Mol. Med*. 60:27–37.

Detter, J.C., Q. Zhang, E.H. Mules, E.K. Novak, V.S. Mishra, E.B. McMurtie, V.T. Tchernev, M.R. Wallace, M.C. Seabra, R.T. Swank, and S.F. Kingsmore. 2000. Rab geranylgeranyl transferase alpha mutation in the gunmetal mouse reduces Rab prenylation and platelet synthesis. *Proc. Natl. Acad. Sci. USA*. 97:4144–4149.

Echard, A., F. Jollivet, O. Martinez, J.J. Lacapere, A. Rousselet, I. Janoueix-Lerosey, and B. Goud. 1998. Interaction of a Golgi-associated kinesin-like protein with Rab6. *Science.* 279:580–585.

Espreafico, E.M., D.E. Coling, V. Tsakraklides, K. Krogh, J.S. Wolenski, G. Kalinec, and B. Kachar. 1998. Localization of myosin-V in the centrosome. *Proc. Natl. Acad. Sci. USA*. 95:8636–8641.

Farnsworth, C.C., M.C. Seabra, L.H. Ericsson, M.H. Gelb, and J.A. Glomset. 1994. Rab geranylgeranyl transferase catalyzes the geranylgeranylation of adjacent cysteines in the small GTPases Rab1A, Rab3A, and Rab5A. *Proc. Natl. Acad. Sci. USA*. 91:11963–11967.

Feig, L.A. 1999. Tools of the trade: use of dominant-inhibitory mutants of Ras-family GTPases. *Nat. Cell Biol*. 1:E25–E27.

Gibson, A., C.E. Futter, S. Maxwell, E.H. Allchin, M. Shipman, J.-P. Kraehenbuhl, D. Domingo, G. Odorizzi, I.S. Trowbridge, and C.R. Hopkins. 1998. Sorting mechanisms regulating membrane protein traffic in the apical transcytotic pathway of polarized MDCK cells. *J. Cell Biol*. 143:81–94.

Guo, W., A. Grant, and P. Novick. 1999. Exo84p is an exocyst protein essential for secretion. *J. Biol. Chem.* 274:23558–23564.

Herz, J., R.C. Kowal, Y.K. Ho, M.S. Brown, and J.C. Goldstein. 1990. Low density lipoprotein receptor-related protein mediates endocytosis of monoclonal antibodies in cultured cells and rabbit liver. *J. Biol. Chem.* 265:21355–21362.

Honing, S., I.V. Sandoval, and K. von Figura. 1998. A di-leucine-based motif in the cytoplasmic tail of LIMP-II and tyrosinase mediates selective binding of AP-3. *EMBO (Eur. Mol. Biol. Organ.) J*. 17:1304–1314.

Jackson, I.J. 1994. Molecular and developmental genetics of mouse coat color. *Annu. Rev. Genet*. 28:189–217.

Jackson, I.J. 1997. Homologous pigmentation mutations in human, mouse and other model organisms. *Hum. Mol. Genet*. 6:1613–1624.

Jimbow, K., J.S. Park, F. Kato, K. Hirosaki, K. Toyofuku, C. Hua, and T. Yamashita. 2000. Assembly, target-signaling and intracellular transport of tyrosinase gene family proteins in the initial stage of melanosome biogenesis. *Pigm. Cell Res.* 13:222–229.

Lee, Z.H., L. Hou, G. Moellmann, E. Kuklinska, K. Antol, M. Fraser, R. Halaban, and B.S. Kwon. 1996. Characterization and subcellular localization of human Pmel 17/silver, a 110-kDa (pre)melanosomal membrane protein associated with 5,6,-dihydroxyindole-2-carboxylic acid (DHICA) converting activity. *J. Invest. Dermatol*. 106:605–610.

McBride, H.M., V. Rybin, C. Murphy, A. Giner, R. Teasdale, and M. Zerial. 1999. Oligomeric complexes link Rab5 effectors with NSF and drive membrane fusion via interactions between EEA1 and syntaxin 13. *Cell.* 98:377–386.

Menasche, G., E. Pastural, J. Feldmann, S. Certain, F. Ersoy, S. Dupuis, N. Wulffraat, D. Bianchi, A. Fischer, F. Le Deist, and G. de Saint Basile. 2000. Mutations in RAB27A cause Griscelli syndrome associated with haemophagocytic syndrome. *Nat. Genet*. 25:173–176.

Mercer, J.A., P.K. Seperack, M.C. Strobel, N.G. Copeland, and N.A. Jenkins. 1991. Novel myosin heavy chain encoded by murine dilute coat colour locus. *Nature.* 349:709–713.

Moore, K.J., D.A. Swing, E.M. Rinchik, M.L. Mucenski, A.M. Buchberg, N.G. Copeland, and N.A. Jenkins. 1988. The murine dilute suppressor gene dsu suppresses the coat-color phenotype of three pigment mutations that alter melanocyte morphology, d, ash and ln. *Genetics.* 119:933–941.

Nagata, K.-i., T. Satoh, H. Itoh, T. Kozasa, Y. Okano, T. Doi, Y. Kaziro, and Y. Nozawa. 1990. The ram: a novel low molecular weight GTP-binding protein cDNA from a rat megakaryocyte library. *FEBS Lett*. 275:29–32.

Nascimento, A.A., T.G. Amaral, J.C. Bizario, R.E. Larson, and E.M. Espreafico. 1997. Subcellular localization of myosin-V in the B16 melanoma cells, a wild-type cell line for the dilute gene. *Mol. Biol. Cell.* 8:1971–1988.

Nielsen, E., F. Severin, J.M. Backer, A.A. Hyman, and M. Zerial. 1999. Rab5 regulates motility of early endosomes on microtubules. *Nat. Cell Biol*. 1:376–382.

Novick, P., and M. Zerial. 1997. The diversity of Rab proteins in vesicle transport. *Curr. Opin. Cell Biol*. 9:496–504.

Orlow, S.J., R.E. Boissy, D.J. Moran, and S. Pifko-Hirst. 1993. Subcellular distribution of tyrosinase related protein-1: implications for melanosomal biogenesis. *J. Invest. Dermatol.* 100:55–64.

Peranen, J., P. Auvinen, H. Virta, R. Wepf, and K. Simons. 1996. Rab8 promotes polarized membrane transport through reorganization of actin and microtubules in fibroblasts. *J. Cell Biol*. 135:153–167.

Pereira-Leal, J.B., and M.C. Seabra. 2000. The mammalian Rab family of small GTPases: definition of family and subfamily sequence motifs suggests a mechanism for functional specificity in the Ras superfamily. *J. Mol. Biol.* 301:1077–1087.

Pfeffer, S.R. 1999. Motivating endosome motility. *Nat. Cell Biol*. 1:E17–E22.

Provance, D.W., Jr., M. Wei, V. Ipe, and J.A. Mercer. 1996. Cultured melanocytes from dilute mutant mice exhibit dendritic morphology and altered melanosome distribution. *Proc. Natl. Acad. Sci. USA*. 93:14554–14558.

Roberts, R.L., M.A. Barbieri, K.M. Pryse, M. Chua, J.H. Morisaki, and P.D. Stahl. 1999. Endosome fusion in living cells overexpressing GFP-rab5. *J. Cell Sci.* 112:3667–3675.

Rogers, S.L., and V.I. Gelfand. 2000. Membrane trafficking, organelle transport, and the cytoskeleton. *Curr. Opin. Cell Biol*. 12:57–62.

Schimmöller, F., I. Simon, and S.R. Pfeffer. 1998. Rab GTPases, directors of vesicle docking. *J. Biol. Chem*. 273:22161–22164.

Seabra, M.C., Y. Reiss, P.J. Casey, M.S. Brown, and J.L. Goldstein. 1991. Protein farnesyltransferase and geranylgeranyltransferase share a common alpha subunit. *Cell*. 65:429–434.

Seabra, M.C., M.S. Brown, C.A. Slaughter, T.C. Südhof, and J.L. Goldstein. 1992. Purification of component A of Rab geranylgeranyl transferase: possible identity with the choroideremia gene product. *Cell*. 70:1049–1057.

Seabra, M.C., M.S. Brown, and J.L. Goldstein. 1993. Retinal degeneration in choroideremia: deficiency of rab geranylgeranyl transferase. *Science.* 259: 377–381.

Seabra, M.C., Y.K. Ho, and J.S. Anant. 1995. Deficient geranylgeranylation of Ram/Rab27 in choroideremia. *J. Biol. Chem*. 270:24420–24427.

Shen, F., and M.C. Seabra. 1996. Mechanism of digeranylgeranylation of Rab proteins. Formation of a complex between monogeranylgeranyl-Rab and Rab escort protein. *J. Biol. Chem.* 271:3692–3698.

Shotelersuk, V., and W.A. Gahl. 1998. Hermansky-Pudlak syndrome: models

for intracellular vesicle formation. *Mol. Genet. Metab*. 65:86–96.
Spritz, R.A. 2000. Hermansky-Pudlak syndrome and pale ear: melanosome-making for the millennium. *Pigm. Cell Res*. 13:15–20.
Stenmark, H., G. Vitale, O. Ullrich, and M. Zerial. 1995. Rabaptin-5 is a direct effector of the small GTPase Rab5 in endocytic membrane fusion. *Cell.* 83: 423–432.
Swank, R.T., E.K. Novak, M.P. McGarry, M.E. Rusiniak, and L. Feng. 1998. Mouse models of Hermansky Pudlak syndrome: a review. *Pigm. Cell Res*. 11:60–80.
Tisdale, E.J., J.R. Bourne, R. Khosravi-Far, C.J. Der, and W.E. Balch. 1992. GTP-binding mutants of rab1 and rab2 are potent inhibitors of vesicular transport from the endoplasmic reticulum to the Golgi complex. *J. Biol. Chem*. 119:749–761.
Tolmachova, T., J.S. Ramalho, J.S. Anant, R.A. Schultz, C.M. Huxley, and M.C. Seabra. 1999. Cloning, mapping and characterization of the human RAB27A gene. *Gene.* 239:109–116.
Tsakraklides, V., K. Krogh, L. Wang, J.C. Bizario, R.E. Larson, E.M. Espreafico, and J.S. Wolenski. 1999. Subcellular localization of GFP-myosin-V in live mouse melanocytes. *J. Cell Sci.* 112:2853–2865.
Valentijn, J.A., K. Valentijn, L.M. Pastore, and J.D. Jamieson. 2000. Actin coating of secretory granules during regulated exocytosis correlates with the release of rab3D. *Proc. Natl. Acad. Sci. USA*. 97:1091–1095.
Vijayasaradhi, S., Y. Xu, B. Bouchard, and A.N. Houghton. 1995. Intracellular sorting and targeting of melanosomal membrane proteins: identification of signals for sorting of the human brown locus protein, gp75. *J. Cell Biol.* 130: 807–820.
Walch-Solimena, C., R.N. Collins, and P.J. Novick. 1997. Sec2p mediates nucleotide exchange on Sec4p and is involved in polarized delivery of post-Golgi vesicles. *J. Cell Biol*. 137:1495–1509.
Walworth, N.C., B. Goud, A.K. Kabcenell, and P.J. Novick. 1989. Mutational analysis of SEC4 suggests a cyclical mechanism for the regulation of vesicular traffic. *EMBO (Eur. Mol. Biol. Organ.) J*. 8:1685–1693.
White, J., L. Johannes, F. Mallard, A. Girod, S. Grill, S. Reinsch, P. Keller, B. Tzschaschel, A. Echard, B. Goud, and E.H.K. Stelzer. 1999. Rab6 coordinates a novel Golgi to ER retrograde transport pathway in live cells. *J. Cell Biol*. 147:743–759.
Wilson, S.M., R. Yip, D.A. Swing, T.N. O'Sullivan, Y. Zhang, E.K. Novak, R.T. Swank, L.B. Russell, N.G. Copeland, and N.A. Jenkins. 2000. A mutation in Rab27a causes the vesicle transport defects observed in ashen mice. *Proc. Natl. Acad. Sci. USA*. 97:7933–7938.
Woodman, P. 1998. Vesicle transport: more work for the Rabs? *Curr. Biol*. 8:R199–R201.
Wu, X., B. Bowers, Q. Wei, B. Kocher, and J.A. Hammer III. 1997. Myosin V associates with melanosomes in mouse melanocytes: evidence that myosin V is an organelle motor. *J. Cell Sci.* 110:847–859.
Wu, X., B. Bowers, K. Rao, Q. Wei, and J.A. Hammer, III. 1998. Visualization of melanosome dynamics within wild-type and dilute melanocytes suggests a paradigm for myosin V function in vivo. *J. Cell Biol*. 143:1899–1918.
Yasamura, Y., A.M. Tashjian, and G.H. Sato. 1966. Establishment of four functional, clonal strains of animal cells in culture. *Science*. 154:1186–1189.